

## 3.5.4 ICRS Centre

### Introduction

The IAU has charged the IERS with the responsibility of monitoring the International Celestial Reference System (ICRS), maintaining its current realization, the International Celestial Reference Frame (ICRF), and maintaining and improving the links with other celestial reference frames. Starting in 2001, these activities have been run jointly by the ICRS Centre (Observatoire de Paris and US Naval Observatory) of the IERS and the International VLBI Service for Geodesy and Astrometry (IVS), in coordination with the IAU. The present report was jointly prepared by the Paris Observatory and US Naval Observatory components of the ICRS Centre. The ICRS Centre web site <<http://hpiers.obspm.fr/icrs-pc>> provides information on the characterization and construction of the ICRF (radio source nomenclature, physical characteristics of radio sources, astrometric behavior of a set of sources, radio source structure). This information is also available by anonymous ftp (<[hpiers.obspm.fr/icrs-pc](ftp://hpiers.obspm.fr/icrs-pc)>), and on request to the ICRS Centre ([icrspc@hpopa.obspm.fr](mailto:icrspc@hpopa.obspm.fr)).

### Maintenance and extension of the ICRF and investigation of future realizations of the ICRS

The International Celestial Reference System (ICRS), adopted by the International Astronomical Union (IAU) in 1997, forms the underlying basis for all astrometry by defining the reference directions of a quasi-inertial celestial coordinate system that are fixed with respect to the most distant objects in the universe. Since 1 January 1998, the ICRS has been realized by the International Celestial Reference Frame (ICRF), which is based on the radio wavelength astrometric positions of compact extragalactic objects determined by the technique of very long baseline interferometry (VLBI).

At the XXVII General Assembly of the IAU held in Rio de Janeiro, Brazil, a second realization of the International Celestial Reference Frame (ICRF2; Fey, Gordon and Jacobs 2009) was adopted as the fundamental celestial reference frame as of 1 January 2010. ICRF2 is again based on the radio wavelength astrometric positions of compact extragalactic objects determined by the technique of VLBI. Significant developments and improvements in geodetic/astrometric VLBI observing and analysis have been made since the initial generation of the ICRF, hereafter ICRF1. Sensitivity of VLBI observing systems to weaker sources and overall data quality have improved significantly due to advances in VLBI receiver and recording systems and due to better observing strategies coordinated by the International VLBI Service for Geodesy and Astrometry (IVS). The use of newer and more modern radio telescopes, such as the 10-station Very Long Baseline Array (VLBA) of the National Radio Astronomy Observatory (NRAO) has also

greatly improved the sensitivity and quality of recent data. Further, enhanced geophysical modeling and computers with faster processors have allowed significant improvements in data analysis techniques and astrometric position estimation.

ICRF2 contains precise positions of 3414 compact extragalactic sources, more than five times the number as in ICRF1. The ICRF2 has a noise floor of approximately 40 micro-arcseconds, some 5–6 times better than ICRF1, and an axis stability of approximately 10 micro-arcseconds, nearly twice as stable as ICRF1. Alignment of ICRF2 with the ICRS was made using 138 stable sources common to both ICRF2 and ICRF1. Maintenance of ICRF2 will be made using a set of 295 new “defining” sources selected on the basis of positional stability and the lack of extensive intrinsic source structure. The stability of these 295 defining sources, and their more uniform sky distribution eliminates the two largest weaknesses of ICRF1.

ICRS Centre personnel are involved in a program to extend the ICRF to higher radio frequencies than those currently used. At these higher radio frequencies, e.g., K-band (24 GHz), Ka-band (32 GHz), and Q-band (43 GHz), contributions to source position uncertainties from intrinsic source structure and from the Earth’s ionosphere will be less than that at the radio frequencies currently used for astrometric/geodetic VLBI. VLBA observations to extend the ICRF to K-band and Q-band continued in 2014. These observations are part of a joint program between the National Aeronautics and Space Administration (NASA), the USNO, the NRAO and Bordeaux Observatory. Preliminary results of these high frequency reference frame observations can be found in Charlot et al. (2010) and Lanyi et al. (2010). Results of observations to determine the position/structure stability of four ICRF2 quasars can be found in Fomalont et al. (2011).

At the IAU General Assembly in Beijing in August 2012, ICRS Centre personnel organized an effort to establish an IAU Working Group on ICRF3. The effort was well received by the IAU. A steering committee was established which met in Beijing and subsequently in October 2012 in Bordeaux. The steering committee wrote a charter for the working group, established Working Group membership, and selected a Working Group chair. The IAU subsequently accepted all these, and formally established the Working Group. In 2014 the ICRF3 Working Group pursued new observations that filled some gaps and improved weaknesses of ICRF2, prepared a progress report to the IAU General Assembly in 2015, and pursue the completion of ICRF3 in 2018.

In the coming decades, there will be significant advances in the area of space-based optical astrometry. Missions such as the European Space Agency’s (ESA) Gaia mission, which launched 19 December 2013, are expected to achieve astrometric positio-

nal accuracies beyond that presently obtained by ground-based radio interferometric measurements. Whether future versions of the ICRF transition back from the radio to the optical depends at least partially upon the relative astrometric accuracy of future radio- and optical-based reference frames.

### Assessment of VLBI realisations of the ICRF

Eight catalogs were submitted respectively by Geoscience Australia (aus2015a/b), the Federal Agency for Cartography and Geodesy (BKG Leipzig) and Institute of Geodesy and Geoinformation of the University of Bonn (IGGB) (bkg2014a), the Space Geodesy Center (CGS) of Matera (cgs2014a), the NASA Goddard Space Flight Center (GSFC) (gsf2014a), the Institute of Applied Astronomy (IAA) of the Russian Academy of Sciences (RAS) (iaa2014a), the Paris Observatory (opa2015a), and the US Naval Observatory (usn2015a). All these catalogs provide right ascension ( $\alpha$ ) and declination ( $\delta$ ) of extragalactic radio sources, as well as their respective uncertainties, the correlation coefficient between  $\alpha$  and  $\delta$ , and the number of sessions and delays. Note that bkg2014a, cgs2014a, gsf2014a, opa2015a, and usn2015a were produced with the same geodetic VLBI analysis software package SOLVE developed at NASA GSFC. Both aus2015a/b and iaa2014a were produced with OCCAM.

Table 1 displays the total number of sources of each catalog, as well as the number of ICRF2 sources (out of 3414) and ICRF2 defining sources (out of 295). Some catalogs do not provide values for one or two defining sources, likely because they do not process a few sessions that were present in the session list processed to generate the ICRF2 catalog. We recommend that in the future, the analysis centers pay attention to their session list in order to get values for all 295 ICRF2 defining sources. As well, none of the catalogs provide values for all 3414 ICRF2 sources.

*Table 1: Number of sources by categories and median error. Unit is  $\mu$ as. Values for right ascension are corrected from the cosine of the declination.*

	----- No. Sources -----			-- Median Error --	
	Total	ICRF2	Def	RA	Dec
aus2015a	3383	3170	295	676.5	965.0
aus2015b	3406	3191	295	576.0	817.0
bkg2014a	3340	3110	294	281.4	429.4
cgs2014a	969	961	294	44.3	50.1
gsf2014a	3740	3408	294	264.0	400.0
iaa2014a	2946	2799	293	445.6	690.3
opa2015a	3684	3378	295	283.5	440.2
usn2015a	4048	3410	295	230.0	333.3

The median error reported in Table 1 reveals an error in declination larger than in right ascension by a factor of  $\sim 1.5$ . The error is substantially smaller for SOLVE solutions. The smaller error for cgs2014a is likely originating in the fact that the solution provides only well observed sources with low positional standard error.

## Frame orientation

We evaluate the consistency of the submitted catalogs with the ICRF2 by modeling the coordinate difference (in the sense catalog minus ICRF2) by a 6-parameter transformation as used at the IERS ICRS Centre in previous comparisons:

$$\begin{aligned} A1 \tan \delta \cos \alpha + A2 \operatorname{tg} \delta \sin \alpha - A3 + DA (\delta - \delta_0) &= \Delta\alpha, \\ -A1 \sin \alpha + A2 \cos \alpha + DD (\delta - \delta_0) + BD &= \Delta\delta, \end{aligned}$$

where  $A1$ ,  $A2$ ,  $A3$  are rotation angles around the X, Y, and Z axes of the celestial reference frame, respectively,  $DA$  and  $DD$  represent linear variations with the declination (which origin  $\delta_0$  can be arbitrarily chosen but was set to zero in this study),  $BD$  is a bias in declination, and  $\Delta\alpha$  and  $\Delta\delta$  coordinate differences between the studied and the ICRF2 catalogs. The 6 parameters were fitted by weighted least squares to the coordinate difference of the defining sources (upper part of Table 2) and ICRF2 sources (lower part of Table 2) found in the catalog. The standard deviation of the offsets to ICRF2 after removal of the systematics of Table 2 is reported in Table 3 together with the median offset.

Though rotations around the X-axis (angle  $A1$ ) remain almost statistically non significant (within 3 sigmas), all catalogs show significant misorientation around  $A2$  larger than  $10 \mu\text{as}$  (4 sigmas). We note also that solutions aus2015a/b show significant misorientation of the frame around the Z-axis close to  $50 \mu\text{as}$  whereas it remains reasonable for other catalogs. The largest deviation from ICRF2 axes is observed for the bias in declination. Values of  $BD$  are indeed significantly larger than those reported in the 2013 Annual Report for solutions bkg2013a and opa2013a (to be compared to bkg2014a, and opa2015a, respectively). Generally, all SOLVE solutions have declination biases larger than  $30 \mu\text{as}$  in absolute value, which is significantly larger than the ICRF2 axis stability of  $10 \mu\text{as}$  measured at the time of the ICRF2 release in 2009 (Fey et al., 2015). This fact may indicate some systematics in source declinations with respect to solutions of the previous years.

## Zonal errors

Figure 1 displays the offset to ICRF2 (in the sense catalog minus ICRF2) averaged over declination bins of 5 degrees. Solutions opa2015a, usn2015a, and bkg2014a exhibit zonal errors characterized by large declination offsets at low declinations, which may reflect the large values of  $BD$  found in the coordinate difference to ICRF2. A similar effect is also visible but less pronounced for cgs2014a and gsf2014a.

### 3.5.4 ICRS Centre

**Table 2: Rotation parameters with respect to ICRF2. A1, A2, A3 and BD are in  $\mu\text{s}$ . DA and DD are in  $\mu\text{s}$  per degree.**

	A1	A2	A3	DA	DD	BD
<b>Defining sources</b>						
aus2015a	2.2	20.9	49.0	-0.2	-0.4	-10.8
+-	3.7	3.7	3.4	0.1	0.1	3.5
aus2015b	1.7	28.9	52.6	-0.7	-0.5	-17.9
+-	3.9	3.9	3.6	0.1	0.1	3.8
bkg2014a	6.4	13.9	-12.6	0.2	0.9	-53.0
+-	3.5	3.4	3.1	0.1	0.1	3.4
cgs2014a	8.6	19.1	-12.1	0.1	0.1	39.6
+-	3.5	3.5	3.2	0.1	0.1	3.5
gsf2014a	-4.6	11.4	-8.8	0.1	0.6	-38.1
+-	3.4	3.4	3.0	0.1	0.1	3.3
iaa2014a	-3.9	12.1	-1.1	-0.1	0.5	1.0
+-	3.7	3.6	3.4	0.1	0.1	3.7
opa2015a	-8.9	18.9	-3.3	0.1	1.0	-57.8
+-	3.4	3.4	3.1	0.1	0.1	3.3
usn2015a	-9.1	18.1	-2.3	0.2	0.9	-50.9
+-	3.4	3.4	3.1	0.1	0.1	3.3
<b>All common sources</b>						
aus2015a	10.0	14.1	38.0	-0.0	-0.3	-6.0
+-	4.4	4.5	4.1	0.2	0.1	4.1
aus2015b	15.7	25.9	38.4	-0.6	-0.4	-15.8
+-	4.7	4.8	4.5	0.2	0.1	4.4
bkg2014a	10.5	16.5	-13.0	0.2	1.0	-53.7
+-	4.5	4.6	4.2	0.2	0.1	4.3
cgs2014a	10.4	18.8	-9.2	0.2	0.3	37.9
+-	4.5	4.6	4.2	0.2	0.1	4.3
gsf2014a	-2.3	14.5	-8.2	0.1	0.7	-36.0
+-	4.5	4.6	4.2	0.2	0.1	4.2
iaa2014a	-0.9	11.3	-1.8	0.1	0.6	-1.7
+-	4.7	4.8	4.4	0.2	0.1	4.6
opa2015a	-3.8	18.7	-8.7	0.1	1.1	-56.3
+-	4.5	4.6	4.2	0.2	0.1	4.2
usn2015a	-4.5	21.2	-8.5	0.0	1.1	-53.4
+-	4.5	4.6	4.2	0.2	0.1	4.2

**Table 3: Statistics after removal of systematics given in Tables 2. Unit is  $\mu\text{s}$ . Values for right ascension are corrected from the cosine of the declination.**

	---- Standard Deviation ----				----- Median Offset -----			
	- Defining -		---- All ----		- Defining -		---- All ----	
	RA	Dec	RA	Dec	RA	Dec	RA	Dec
aus2015a	165.0	130.4	165.3	132.1	256.4	419.6	267.9	427.4
aus2015b	68.8	69.2	107.2	119.2	261.1	495.4	264.9	409.8
bkg2014a	48.3	59.4	401.2	419.1	117.3	223.1	118.9	211.4
cgs2014a	47.8	58.9	282.1	520.5	48.9	72.4	50.7	67.0
gsf2014a	48.7	57.1	517.9	771.1	78.7	143.8	79.1	132.8
iaa2014a	49.6	60.9	310.6	304.3	35.6	34.7	180.6	253.5
opa2015a	56.6	62.2	491.5	718.6	51.8	76.5	54.7	82.5
usn2015a	56.7	63.1	546.1	774.4	119.4	232.8	124.6	219.2

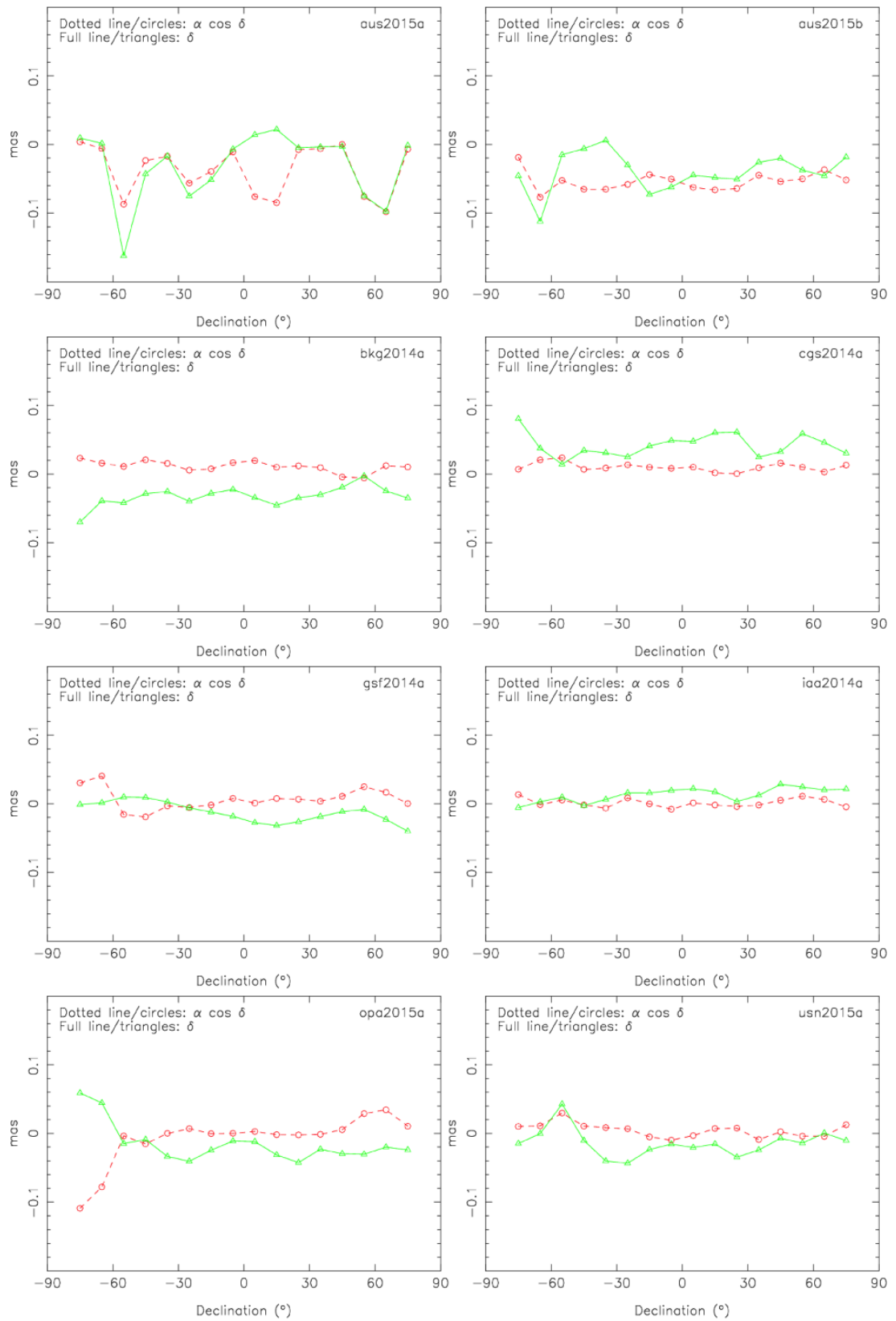


Fig. 1: Offset to ICRF2 for right ascension (dotted line with circles) and declination (full line with triangles) by bins of declination of 5 degrees.

**Standard error and noise**

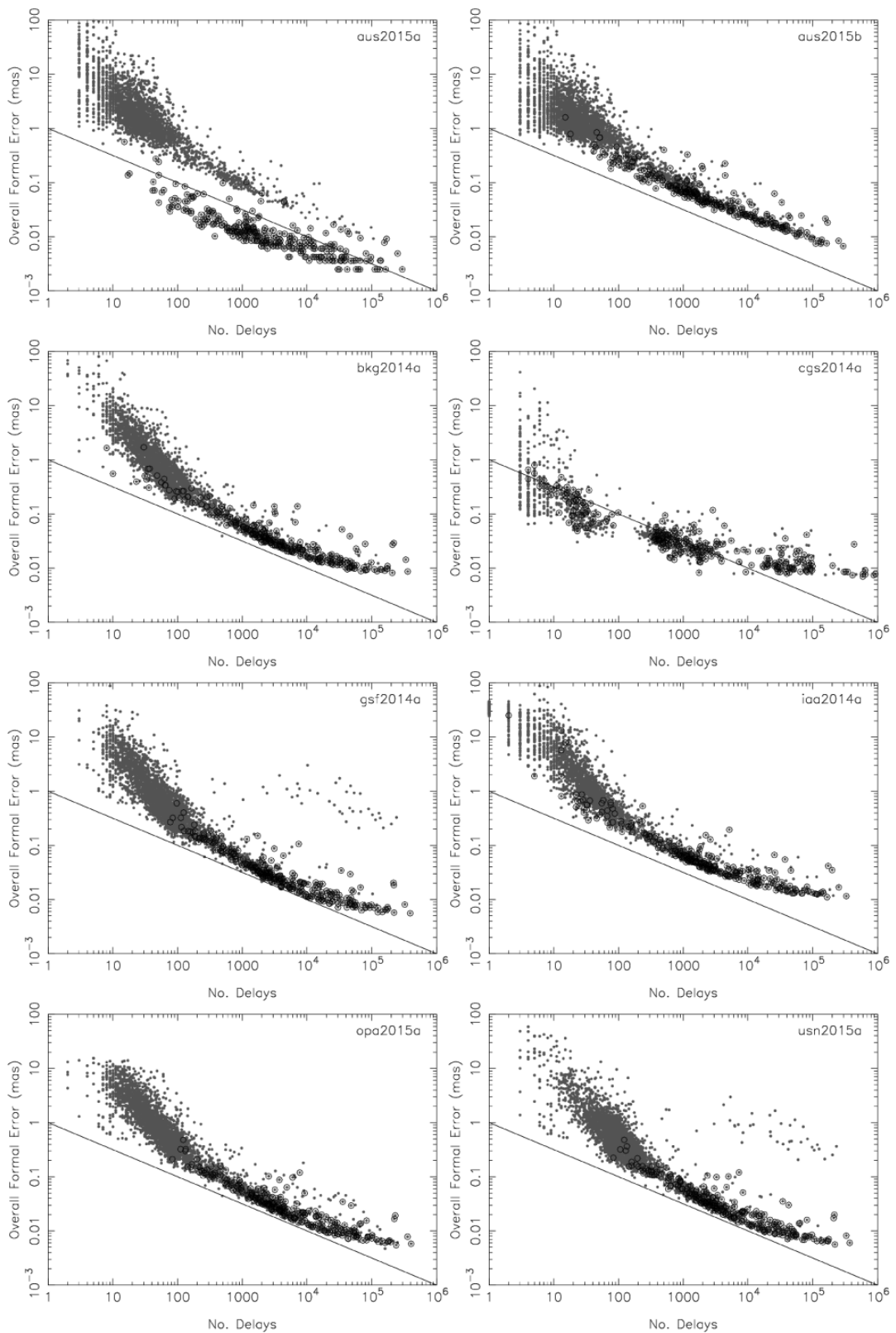
Figure 2 illustrates how the overall formal error, defined as the square root of  $\sigma_{\alpha \cos \delta}^2 + \sigma_{\delta}^2 + c \sigma_{\alpha \cos \delta} \sigma_{\alpha \delta}$  where  $\sigma$  is the formal error listed in the catalogs and  $c$  is the correlation coefficient between estimates of  $\alpha$  and  $\delta$  as provided in the catalogues, varies with the number  $N$  of observations. The circled dots represent defining sources. The figure for aus2015a clearly shows that the defining sources have underestimated formal errors likely due to an over-constrained solution. (As stated in the technical document delivered with the catalog, a strong no-net rotation condition imposed to these sources.) The formal error of the same sources in solution aus2015b, in which the no-net rotation condition is less severe, appears to be at a level comparable to other sources.

Figure 2 also shows how the error on delays is propagated to the estimated source coordinates. For white noise measurements, the formal error on source coordinates is expected to decrease as  $N^{-0.5}$ . The figure reveals that this regime exists for  $N$  between  $\sim 100$  and  $\sim 10000$ . For  $N$  lower than a hundred observations (e.g., VCS sources or sources observed in only one session) the formal error varies as  $N^{-1}$ . Beyond 10000 observations, the formal error generally tends towards a limit lower than  $\sim 10 \mu\text{as}$ . Such a deviation is visible for all catalogs except aus2015a/b for which the formal error seems to continue to decrease closely to  $N^{-0.5}$ . The deviation for large  $N$  observed for all other catalogs is likely the signature of non-Gaussian correlated errors: as  $N$  increases, thermal baseline-dependent error tends to zero and the station-dependent error arising from time- and space-correlated parameters becomes dominant (see, e.g., Gipson 2006 or Romero-Wolf et al. 2012).

A last test was performed to assess the consistency between the formal errors and the offset to ICRF2. This test was motivated by the consideration that, although the ICRF2 is not the “truth”, it nevertheless provides accurate values of well-observed sources. As a consequence, for most of the sources, the addition of new observations after 2009 should not perturb significantly the estimated position but only improve the formal error. For formal errors lower than 0.1 mas, one sees that the scatter is over the diagonal, indicating a possible underestimation of the formal errors. To quantify this scale factor, one can estimate it together with an error floor so that a realistic error  $E_r$  (i.e., that explains the observed offset to ICRF2) is given by

$$E_r = ((E s)^2 + f^2)^{0.5}$$

where  $E$  is the error,  $s$  a scale factor and  $f$  a noise floor. Values of  $s$  and  $f$  estimated over sources whose offset to ICRF2 is smaller than 1 mas are reported in Table 4. Uncertainties are  $\sim 10 \mu\text{as}$  on  $f$  and  $\sim 0.01$  on  $s$ . SOLVE solutions tend to have scale factors larger than unity while OCCAM catalogs have scale factors smaller than 1. Note that the noise floor does not represent the catalog



*Fig. 2: Overall formal error as a function of the number of observations. The circled dots represent defining sources. The solid line indicates a decrease as  $N^{-1/2}$  where  $N$  is the number of delays.*

*Table 4: Noise floor ( $\mu\text{as}$ ) and scale factor estimated for sources with offset lower than 1 mas. Values for right ascension are corrected from the cosine of the declination.*

	-- Floor --		-- Scale --	
	RA	Dec	RA	Dec
aus2015a	97.3	117.5	0.79	0.79
aus2015b	70.4	71.2	0.96	0.93
bkg2014a	45.6	62.5	1.26	1.11
cgs2014a	36.4	48.7	2.70	2.38
gsf2014a	47.7	60.3	1.14	1.06
iaa2014a	44.4	52.1	0.99	0.83
opa2015a	50.8	62.4	1.27	1.11
usn2015a	53.7	65.6	1.67	1.47

internal error since one considers the offset to ICRF2: the quantity  $f$  therefore contains the internal noise of the ICRF2. The global noise lies between 50 and 120  $\mu\text{as}$ . If one assumes 40  $\mu\text{as}$  for the ICRF2 internal noise (Fey et al., 2015), it means that the analyzed catalog internal noises are larger by a factor between 1 and 3.

### Conclusions and recommendations

The above results lead to some recommendations for analysis centers who plan new submissions in the future. First, it is recommended to include all ICRF2 sources in the processed session list, in order to get values of, at least, all 3414 ICRF2 sources. Second, analysis centers should focus on understanding several points: (i) the significant systematics in orientation ( $\sim 50 \mu\text{as}$ ) showing up in Table 2, (ii) the zonal errors appearing in Fig. 1 for some solutions, and (iii) the non-Gaussian errors dominating for large number of observations discussed previously. About the latter item, one should understand particularly why aus2015a/b OCCAM solutions decreases differently than SOLVE catalogs for larger numbers of delays. In the future, the correction of this defect should be achieved by better modeling and parameterization of clock and troposphere correlated errors (Lambert 2014).

### Monitor source structure to assess astrometric quality

#### The Radio Reference Frame Image Database

The Radio Reference Frame Image Database (RRFID) is a web accessible database of radio frequency images of ICRF sources. The RRFID currently contains 7279 VLBA images of 782 sources at radio frequencies of 2.3 GHz and 8.4 GHz. Additionally, the RRFID contains 1867 images of 285 sources at frequencies of 24 GHz and 43 GHz. Imaging of additional radio sources has been temporarily suspended due to lack of available resources. The RRFID can be accessed from the Analysis Center web page or directly at <http://rorf.usno.navy.mil/rrfid.shtml>.

**The Bordeaux VLBI Image Database**

The Bordeaux VLBI Image Database (BVID) is a web accessible database of radio frequency images of ICRF sources. The BVID currently contains more than 3500 VLBA images of 1100 sources mostly at radio frequencies of 2.3 GHz and 8.4 GHz, but includes images for some sources at 24 GHz and 42 GHz. The BVID can be accessed from the Analysis Center web page or directly at <http://www.obs.u-bordeaux1.fr/BVID/>.

**Linking the ICRF to frames at other wavelengths**

The link between the ICRF and other celestial reference frames is fundamental to prepare the future ICRF as well as the future connection between the ICRS and the GCRS (Gaia Celestial Reference System). During the reporting period (2014) ICRS Centre personnel continued to make progress with several astrometric star catalogs (e.g URAT), the extragalactic link to ICRF sources, and the preparation for the Gaia astrometric space mission.

**Optical Representation of the ICRS: Gaia**

The ICRS/ICRF paradigm is based on a frame formed by very distant extragalactic sources that is assumed to have no global rotation. By definition, this frame is considered to be kinematically non-rotating. To present date the versions of the ICRF (IERS Tech. Notes 23/1997 and 35/2009) were formed by VLBI positions of selected radio-loud quasars. The Gaia astrometric solution will be referred to a kinematically non-rotating frame thanks to the global zero-proper motion constraint set on the clean subset of quasars detected by Gaia. The positional accuracy of the individual sources will depend on their magnitude, but at least for the (forecasted) 30,000 QSOs brighter than  $G=18$  this would be better than 80  $\mu\text{as}$  and 60  $\mu\text{as/yr}$  formal error per source coordinate (position and proper motion, respectively). This astrometric solution should supersede the VLBI based versions of the ICRF, and bring the primary representation of the ICRS to the optical wavelength at the time of issuing of the Gaia final solution, to be published around 2020 (Mignard, 2012). In preparation for what is currently called the Gaia Celestial Reference Frame (GCRF), the Gaia Initial QSO Catalog has been prepared (Andrei et al., 2012a,b).

**The Gaia Initial QSO Catalog (GIQC)**

The latest version of the Gaia Initial QSO Catalog (GIQC) produced by the Gaia Coordination Unit 3 (CU3), workpackage GWP-S-335-13000, contains 1,248,372 objects, of which 191,372 are considered and marked as “defining” ones, because of their observational history and the existence of spectroscopic redshift. Also objects with strong, calibrator-like radio emission are included in this category. The “defining” objects represent a clean sample of quasars. The remaining objects aim to bring completeness to the GIQC at the time of its compilation. For the whole GIQC the average density is 30.3 sources per sq.deg. Practically all sources

have an indication of magnitude and of morphological indexes, and 90% of the sources have an indication of redshift and of variability indexes. Besides presenting morphological variability, and classification indexes (plus a one-letter comment on the source main feature), the GIQC is being used to define the astrometric reference frame for the 2016 release of the preliminary Gaia catalog. QSOs are used as well for surveillance of stability of the measurements. The GIQC was part of two publications: Smart & Nicastro, A&A vol. 570 pp. 87 (tables at CDS); Michalik et al., A&A in preparation.

#### ***Optical Images of the QSOs linking the VLBI and the Gaia Celestial Reference frames***

The connection between the International Celestial Reference Frame, currently defined by Very Long Baseline Interferometry (VLBI) observations of quasars, and the future Gaia Celestial Reference Frame (GCRF) is demanded for continuity reasons, since it is foreseen that the GCRF will be the future materialization of the International Celestial Reference System. Each quasar candidate to be used for this alignment should be scrutinized so that the ones that are retained for the link represent the top precision astrometry that can be reached by VLBI and Gaia observations. On the VLBI side specific observations are already being made. In the optical window long term campaigns follow the sources variability (see more on this topic elsewhere in this report). The program obtains optical images with high SNR, using preferably the B and R Johnson filters, for the candidate sources appropriate for the link. The main goal is to establish whether there is an apparent underlying host galaxy, and to which level are the corresponding isophotes. If prominent, the source must be flagged in the Gaia observations, because its centroid ought to be determined with special care for the sake of precision and to be properly compared against the VLBI centroid.

At this point there are already collected good quality images of the optical counterpart of QSOs – in particular the ICRF sources, with special effort toward those that have been regularly radio surveyed either for future implementation at high frequencies and/or those that will be the link sources between the ICRF and the Gaia CRF. Observations have been taken at the LNA/Brazil, CASLEO/Argentina, NOT/Spain, LFOA/Austria, Rozhen/Bulgária, and ASV/Serbia. In complement images are also collected from the Sloan Digital Sky Survey (SDSS) and from the Digitized Sky Surveys (DSS). An image data bank is planned to be made publicly available through the IERS ICRS Centre. The photometry analysis is centred on the morphology, since there remain still cases in which the host galaxy is overwhelming, and many cases in which a non-stellar PSF modelling is required. On basis of the neighbour stars we assign magnitudes and variability whenever

possible. Moreover, since Gaia will not obtain direct images of the observed sources, the morphology and magnitude becomes useful as templates onto which assembling and interpreting the one-dimensional and uncontinuous line spread function samplings that will be delivered by Gaia for each QSO.

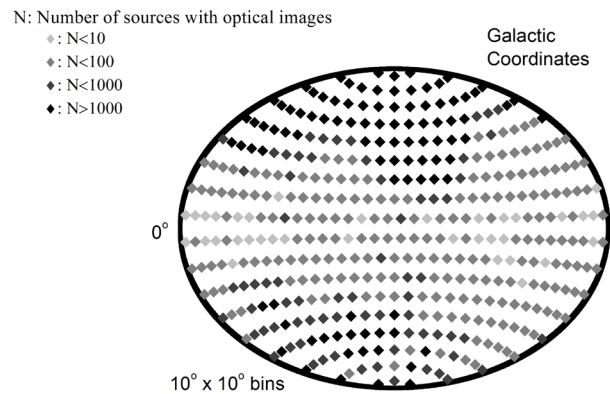


*Fig. 3: Sky distribution of the QSOs for which specific observations were made by this program – that is, the images from the SDSS and the DSS do not appear in this plot.*

An observational program for identification of the reference sources in radio/optical has also continued at several large optical facilities (PI: Oleg Titov). This program focuses on the future link between the radio reference frame produced by VLBI and the optical reference frame which will be produced by Gaia, and comprises several large optical facilities: 3.58-meter New Technology Telescope (NTT, ESO) in Chile; 2.5-meter Nordic Optical Telescope at Canary Islands (NOT) in Spain; two 8-meter Gemini Telescopes in Chile and Hawaii. Spectroscopic observations at optical wavelengths of the reference radio sources to determine redshifts, and, thus, confirm their extragalactic nature are undertaken. Redshifts of ~300 reference radio sources have been measured to date. They were added to the OCARS database (<[http://www.gao.spb.ru/english/as/ac\\_vlbi/ocars.txt](http://www.gao.spb.ru/english/as/ac_vlbi/ocars.txt)>).

### ***The morphology indexes***

In the GIQC as well as in the LQAC (see below) morphological indexes were assigned to each object on basis of the departure of the images from a purely stellar PSF, defined by the stars nearby to each quasar. A morphological departure indicates that the isophotes from the host galaxy must be considered in order to reach maximum precision in the determination of the centroid of the target. A pilot study compared 1,343 quasars in images from the SDSS (r images) and the DSS (R plates). The outcome has shown that the DSS images were able to detect quasars for which the host galaxy signature was sensed in the SDSS images, using the SHARP, SROUND, and GROUND, PSF parameters in IRAF's DAOFIND task. Thus the images of all quasars in the GIQC were

*Table 5: Telescope and filter origins of the sources depicted in the plot. Also shown the available contents of the ICRF2 and the GIQC.*

Country	Brasil	Brasil	Áustria	Bulgaria	Spain	Argentina	Chile
Telescope aperture	1.6m	0.6m	2m	0.6m	2m	2.2m	2.2m
N QSOs	350	495	12	133	190	103	497
Average <Nobs>	6	5	6	35	9	8	8
Magnitude	327	462	12	128	190	6	497
Redshift	281	403	11	123	179	6	404
GIQC-def	305	412	11	121	160	2	180
GIQC-can	11	15	0	1	2	0	19
GIQC-other	34	68	1	11	28	4	298
ICRF2-def	107	150	11	55	62	0	10
ICRF2-vcs	5	7	0	0	2	0	52
ICRF2- non vcs	185	238	0	63	34	0	29
Non ICRF2	53	100	1	15	92	103	406
u	0	0	0	0	0	0	0
B	0	49	0	0	183	94	497
g	0	0	0	0	0	0	0
V	278	413	12	0	0	1	0
C	101	92	0	133	6	0	0
R	36	48	12	0	183	102	497
I	8	0	0	0	0		0

searched for in the B, R, and I plates of the DSS. For each of the 3 DAOFIND parameters, in each of the 3 colors, a morphological index was produced as the z-ratio of the parameter value for the quasar to the mean parameter ratio for the surrounding stars, normalized by the standard deviation in that mean. Thus, in all, there are up to 9 morphological indexes for each quasar. Typically about 10% of the quasars are found with departures larger than 2 in the z-ratio. The departures are clearly more important in the R plates than in the B plates (Souhay et al., 2012).

#### ***The variability indexes***

Variability is a prominent characteristic of quasars, mostly due to the violent processes of infall of matter to the massive central black hole (Taris et al., 2012b). As the objects that will materialize the GCRF will be those with the most accurate and stable positions (which are therefore critical, defining, properties), there is evidence that flux variations at different time scales correlate with variations of the astrometric location of their photocentres. Therefore, photocentre angular variations at different wavelengths are possibly

the results of common phenomena occurring in the vicinity of the central engine of QSOs: the base of relativistic jets, the broad emission line regions, or accretion disks (Popovic et al., 2012).

Typically Gaia will take about 80 measurements of each quasar during the five years mission, a couple of times in successive fields (or slightly more if the quasar happens to occupy the nodus of a transit great circle), and then come back to the target after a month and a half. Such cadence is very well suited to single out the peculiar quasar variability in comparison to other variable sources (Kelly et al., 2009; Andrei et al., 2012c). At the same time, if an associated astrometric jitter is not accounted for, the error budget of the quasar increases beyond what can be attributed to photon noise.

Accordingly variability indexes were produced on basis of the mass of the central black hole and the absolute luminosity of the quasar. With these elements the radius of the accretion disk and that of the dust torus region were calculated, as apparent angular sizes accounting for the cosmological redshift correction. Those two radii, the accretion disk one in micro-arcseconds and the torus one in milli-arcseconds, are given as the indexes to indicate the likeness of an astrometric jitter that would impact the stability of the centroid during the Gaia mission.

***Optical monitoring of extragalactic radiosources to ensure the link between ICRF and the future Gaia celestial reference frame***

After four years of observation, a huge amount of optical images of some AGN's selected to ensure the link between the ICRF and the future Gaia celestial reference frame have been gathered (without taking into account the data mining). They come from small robotic telescopes, medium size or large optical facilities spread all over the world. In 2014 four large telescopes (CFHT, NOT, MPG 2.2 and Rozhen 2m) provided high resolution optical images dedicated to morphology analysis while four smaller ones (OHP, the two TAROT and Zadko) provided images dedicated to photometry. The first results of the optical monitoring campaign were published (Taris et al., 2012a, 2013).

All the optical images will be made available to the astronomers by means of a database currently under construction in the frame of the ICRS Centre. These observations will be also of interest in the context of the Gaia Initial QSO Catalogue (GIQC) and for astrophysical studies (emission regions, gravitational lensing, photocenter scattering, constraints for binary black holes models).

***The Large Quasar Astrometric Catalog***

The ICRS Centre is in charge of the LQAC (Large Quasar Astrometric Catalog), a whole sky compilation of information on known QSOs, as well as of its regular up-dates. The second release of the LQAC, LQAC-2 (Souhay et al., 2012), was published as a CDS catalog. It contained 187,504 quasars. A third release, LQAC-3,

is in preparation in 2014. Its publication is scheduled for the end of 2015. Basically, the LQAC delivers complete information (when available) as a set of optical magnitudes and radio fluxes, the redshift, original and consolidated equatorial coordinates, together with re-calculated absolute magnitudes and morphological indexes (see IERS Annual Report, 2010, 2012).

#### **Link Between Optical and Radio Reference Frames**

Work continued to assess the potential magnitude and explanation for offsets in position between extra-galactic reference frame objects in the optical and in the radio. Analysis of data obtained at CTIO from 1997 to 2004 that used a combination of simultaneous UCAC astrophotograph and CTIO 0.9 m observations in the same bandpass, indicates systematic differences in positions between the optical and radio positions of ICRF2 sources exceeding 100 mas in some cases with suspected general, random offsets of most sources of order single mas (see Zacharias and Zacharias, 2014). If this new and potentially significant source of error holds for alignment sources common to both Gaia and the ICRF, then the optical/radio system alignment error of a significant fraction of a milliarcsecond could result. Results of the reference frame link work were presented at the Extra-Galactic Science with Gaia (EGSG) meeting, held at Observatoire de Paris-Meudon. Additional analysis of this issue, along with new optical and radio observations will be conducted in 2015 and beyond, and the results communicated to the Gaia team and ICRF3 working group.

It is important to keep in mind that the angular resolution of Gaia is about 10 times higher than the ground-based optical morphology investigations mentioned above. Therefore Gaia “sees” a different “blob” of light (AGN core area + host galaxy) than those ground-based imaging data which, in turn, is different from what is seen at radio wavelengths.

A completely different approach for the link between the Gaia (optical) and current ICRF (radio VLBI based) reference frames has been suggested (Zacharias & Zacharias, 2014) in case the link via QSOs is found to be insufficient. Observations of thermal radiation of ordinary stars with ALMA are planned and a positional accuracy on the mas level per star is estimated (Fomalont, priv. com.). Stars, although subject to proper motions, could in principle provide the desired reference frame link between the GCRF and ICRF because the Gaia internal observations are already inertial (non-rotating due to observations of QSOs and galaxies). The radio observations of stars would allow alignment of the positional zero-point of the coordinate systems.

#### **ICRF2 Work**

ICRF2 work continued, with the ICRF2 journal paper nearing completion. The ICRF2 journal paper will be published in 2015.

**URAT1 Catalog release**

The USNO Robotic Astrometric Telescope (URAT) astrometry program continued its northern hemisphere observations. The first 2 years of data (Fig. 4) were reduced and validated using both external and internal (USNO) references for comparison. The first catalog release (URAT1), scheduled for early 2015, will include data for approximately 228 million primarily northern hemisphere (DEC north of  $-15$  deg) stars spanning the magnitude range of  $R=3-18.5$ . Validation using ICRF2 counterparts in the visible indicates systematic errors at or below the 10 mas level (see Fig. 5), with random error estimated at between 5 and 30 mas, as a function of magnitude due to signal-to-noise levels. URAT1 represents the most accurate star catalog released to date that covers hundreds of millions of stars; field “beta” testers (including asteroid occultation observers) report significant improvements in their results have been obtained by using URAT1 in place of UCAC4. Sky coverage of URAT observations were extended to include the area around Pluto in support of NASA’s Pluto fly-by mission “New Horizons”. These data will be incorporated into the URAT1 catalog.

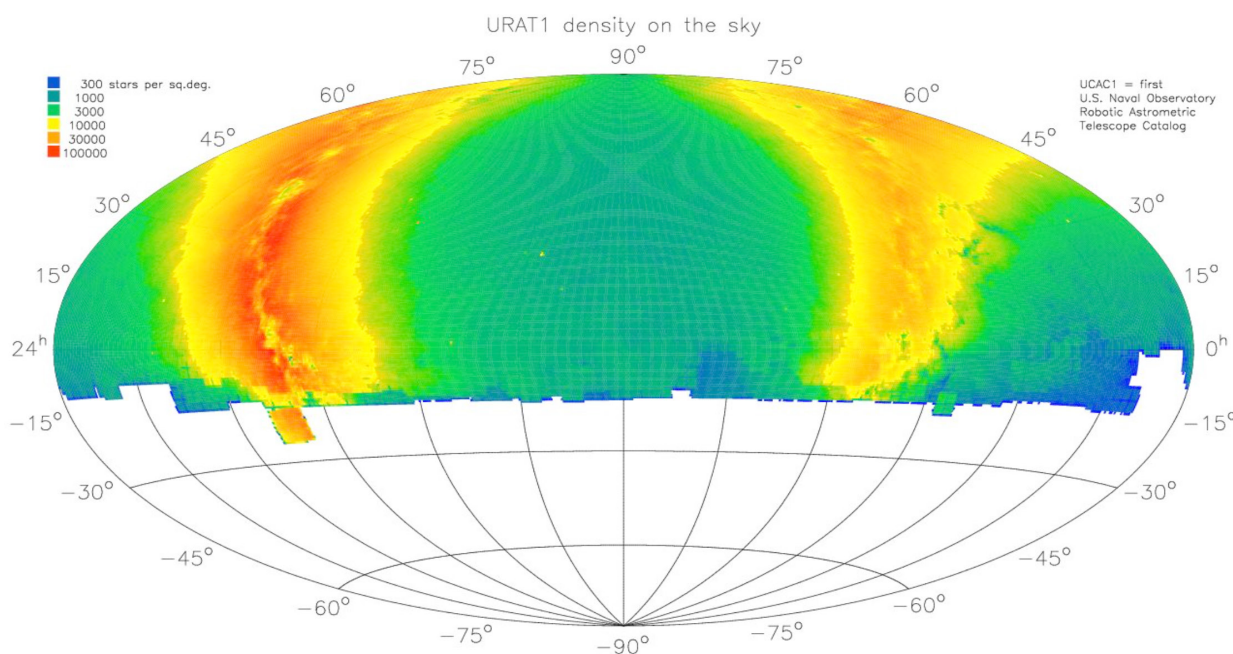


*Fig. 4: URAT sky coverage as of late 2014. The 2015 URAT1 release will consist of approximately 228 million stars covering the sky north of approximately  $-15$  deg DEC. URAT1 includes observations from April 2012 to June 2014, along with extensive validation using a variety of sources.*

### 3.5.4 ICRS Centre

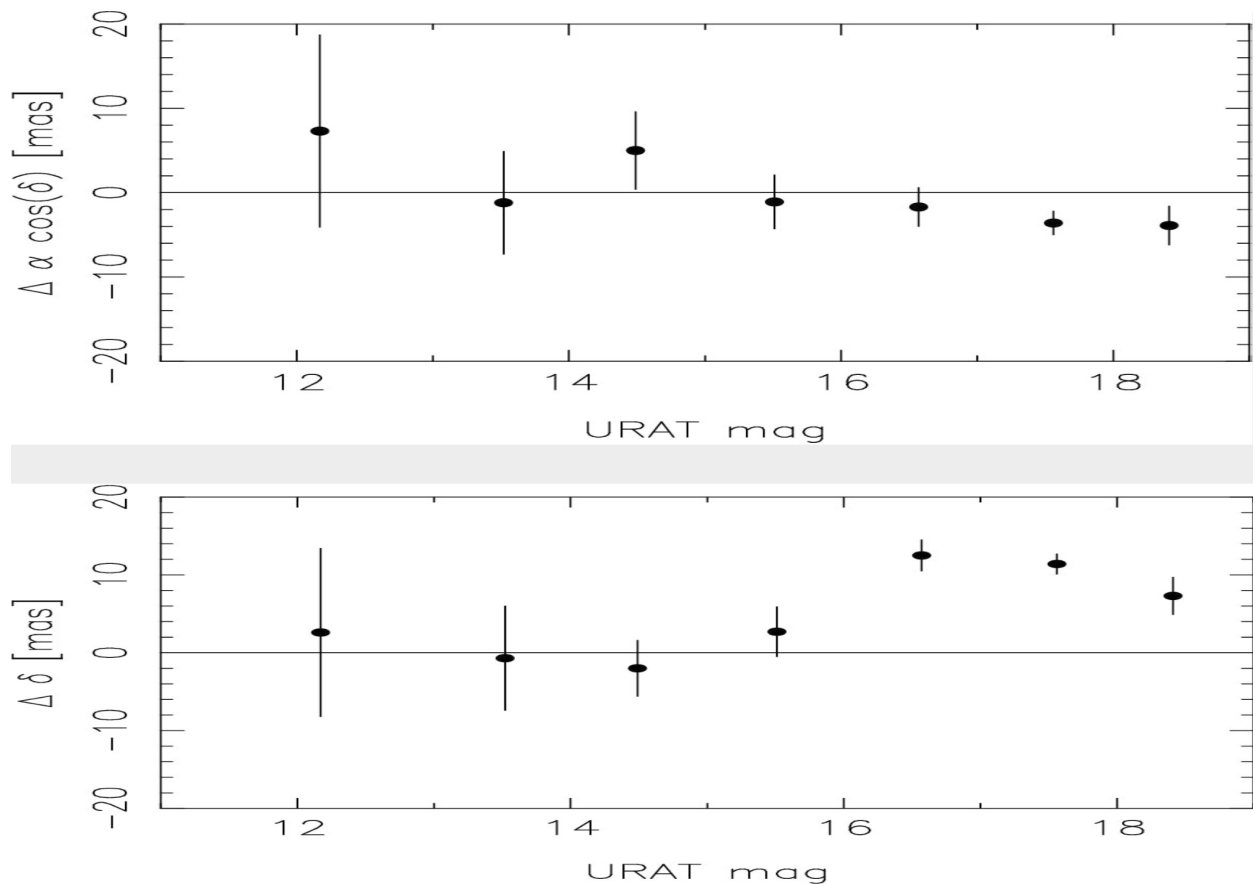


Fig. 5: Differences between URAT1 and ICRF2 sources. Oval indicates mean for all sources in magnitude bin; span indicates sample deviation. (Top) RA cos(DEC); (bottom) Dec. The data are consistent with URAT1 systematic errors at the 10 mas or smaller level.

The URAT1 catalog will be released electronically in 2015 along with an accompanying journal article describing the instrument, data reduction methodology and validation results. Future work will include release of additional northern hemisphere data, and deployment of a modified URAT telescope to the southern hemisphere to conduct a bright star (magnitude range  $R = -1.5$ – $17$ ) survey over the 2015–2016 time period. The URAT data will be used to supplement Gaia optical data for the brightest stars, and will serve as the preferred current epoch optical catalog until the future release of the Gaia catalog covering the same magnitude range at better astrometric accuracies (currently planned for the 2017–2018 timeframe). Eventually, it is anticipated that URAT data will be superseded by Gaia results except at the bright end.

**Staff** Dorland, Bryan, Director (USNO)  
 Souchay, Jean, Co-director (OP)  
 Andrei, Alexandre, Assoc. Astronomer (OP, Obs. Nat. Rio, Brasil)  
 Arias, E. Felicitas, Assoc. Astronomer (BIPM / OP)  
 Barache, Christophe, Engineer (OP)  
 Bouquillon, Sébastien, Astronomer (OP)  
 Fey, Alan, Astronomer (USNO)  
 Lambert, Sébastien, Astronomer (OP)  
 Taris, François, Technician (OP)  
 Titov, Oleg, Astronomer (OP, Geoscience Australia)  
 Zacharias, Norbert, Astronomer (USNO)

**References** Andrei, A. H.; Anton, S.; Barache, C.; Bouquillon, S.; Bourda, G.;  
 Le Campion, J.-F.; Charlot, P.; Lambert, S.; Pereira Osorio, J.  
 J.; Souchay, J.; Taris, F.; Assafin, M.; Camargo, J. I. B.; da Silva  
 Neto, D. N.; Vieira Martins, R.; 2012a; SF2A-2012: Proceedings  
 of the Annual meeting of the French Society of Astronomy and  
 Astrophysics. Eds.: S. Boissier, P. de Laverny, N. Nardetto, R.  
 Samadi, D. Valls-Gabaud and H. Wozniak, pp. 61–66  
 Andrei, A. H.; Anton, S.; Barache, C.; Bouquillon, S.; Bourda, G.;  
 Le Campion, J.-F.; Charlot, P.; Lambert, S.; Pereira Osorio, J.  
 J.; Souchay, J.; Taris, F.; Assafin, M.; Camargo, J. I. B.; da Silva  
 Neto, D. N.; Vieira Martins, R.; 2012b; *Memorie della Societa  
 Astronomica Italiana*, v. 83, p. 930  
 Andrei, Alexandre Humberto; Souchay, Jean; Martins, Roberto  
 Vieira; Anton, Sonia; Taris, Francois; Bouquillon, Sebastien;  
 Assafin, Marcelo; Barache, Christophe; Camargo, Julio Ignac-  
 io Bueno; Coelho, Bruno; da Silva Neto, Dario Nepomuceno;  
 2012c; IAU Joint Discussion 7: Space-Time Reference Systems  
 for Future Research at IAU General Assembly, Beijing. Online at  
 <<http://referencesystems.info/iau-joint-discussion-7.html>, id.31>  
 IERS Technical Note No. 23; 1997; C. Ma and M. Feissel (eds.):  
 Definition and realization of the International Celestial Reference  
 System by VLBI astrometry of extragalactic objects  
 IERS Technical Note No. 35; 2009; Alan L. Fey, David Gordon,  
 and Christopher S. Jacobs (eds.): *The Second Realization of the  
 International Celestial Reference Frame by Very Long Baseline  
 Interferometry*  
 Kelly, B.C., Bechtold, J., Siemiginowska, A.; 2009; *Astrophysical  
 Journal* 698, 895.  
 Michalik, D.; Lindegren, L.; 2014; arXiv:1511.01896.  
 Popovic, L. C.; Jovanovic, P.; Stalevski, M.; Anton, S.; Andrei, A.  
 H.; Kovacevic, J.; Baes, M.; 2012; *Astronomy & Astrophysics*  
 538, id. A107, 11 pp.  
 Smart, R. L.; Nicastro, L.; 2014; *Astronomy & Astrophysics* 570,  
 id. A87.

### 3.5.4 ICRS Centre

Souchay, J.; Andrei, A. H.; Barache, C.; Bouquillon, S.; Suchet, D.; Taris, F.; Peralta, R.; 2012; *Astronomy & Astrophysics* 537, id. A99, 13 pp.

Taris, François; Andrei, Alexandre; Anton, Sonia; Barache, Christophe; Coelho, Bruno; Klotz, Alain; Lambert, Sébastien; Souchay, Jean; Vachier, Frédéric; 2012a; IAU Joint Discussion 7: Space-Time Reference Systems for Future Research at IAU General Assembly-Beijing. Online at <<http://referencesystems.info/iau-joint-discussion-7.html>>, id. P9

Taris, F.; Andrei, A.; Souchay, J.; Klotz, A.; Vachier, F.; Bouquillon, S.; Anton, S.; Côte, R.; Suchet, D. ; 2012b; *Memorie della Societa Astronomica Italiana* 83, p. 986

Taris, F., Andrei, A.H., Klotz, A.; Vachier, F.; Côte, R.; Bouquillon, S.; Souchay, J.; Lambert, S.; Anton, S.; Bourda, G.; Coward, D.; 2013; *Astronomy & Astrophysics* 552, id. A98

Zacharias, N. & Zacharias, M.; 2014, *Astronomical Journal* 147, 95

*Bryan Dorland, Jean Souchay, Alexandre Andrei,  
E. Felicitas Arias, Christophe Barache,  
Sébastien Bouquillon, Alan Fey, Sébastien Lambert,  
François Taris, Oleg Titov, Norbert Zacharias*